

Distinct regulation of histone H3 methylation at lysines 27 and 9 by CpG methylation in *Arabidopsis*

Olivier Mathieu^{1,*}, Aline V. Probst^{1,2}
and Jerzy Paszkowski

Laboratory of Plant Genetics, University of Geneva, Geneva, Switzerland

Transcriptional activity and structure of chromatin are correlated with patterns of covalent DNA and histone modification. Previous studies have revealed that high levels of histone H3 dimethylation at lysine 9 (H3K9me2), characteristic of transcriptionally silent heterochromatin in *Arabidopsis*, require hypermethylation of DNA at CpG sites. Here, we report that CpG hypermethylation characteristic of heterochromatin specifically prevented H3K27 trimethylation (H3K27me3). H3K27 mono- and dimethylation mark silent heterochromatin independently of DNA methylation. Upon loss of CpG methylation, there was target-specific enrichment of H3K27me3 in heterochromatin that correlated with transcriptional reactivation. Moreover, using the *kyp* mutant affected in H3K9me2, we showed that changes in H3K27me3 occurred independently of the levels of H3K9me2. Therefore, CpG methylation provides distinct and direct information for a specific subset of histone methylation marks. The observed independence of the regulation of H3K9 and H3K27 methylation by CpG methylation refines the recently proposed combinatorial histone code involving these two marks.

The EMBO Journal (2005) 24, 2783–2791. doi:10.1038/sj.emboj.7600743; Published online 7 July 2005

Subject Categories: chromatin & transcription; plant biology
Keywords: CpG methylation; histone H3 lysine 27; histone code; silent chromatin

Introduction

Alternative chromatin properties provide permissive or repressive environments for gene expression and these are often correlated with patterns of covalent modifications affecting DNA and histone proteins. The N-terminal ‘tails’ of histones are subject to a variety of post-translational modifications including methylation, acetylation, phosphorylation, ubiquitination, ADP-ribosylation and sumoylation

*Corresponding author. Laboratory of Plant Genetics, University of Geneva, Sciences III, 30 Quai Ernest Ansermet, 1211 Geneva 4, Switzerland. Tel.: +41 22 379 3026; Fax: +41 22 379 3107; E-mail: olivier.mathieu@bioveg.unige.ch

¹These authors contributed equally to this work

²Present address: Laboratory of Nuclear Dynamics and Genome Plasticity, UMR 218 CNRS/Institute Curie, 26 rue d’Ulm, 75248 Paris Cedex 5, France

Received: 6 April 2005; accepted: 15 June 2005; published online: 7 July 2005

(for reviews see Jenuwein and Allis, 2001; Berger, 2002). It has been assumed that the combination of DNA and histone modification specifies chromatin structure and subsequently determines its transcriptional competence (Jenuwein and Allis, 2001). In this respect, functional links between DNA and histone methylation, as the most stable covalent modifications, have received particular attention. Although it was noted more than 30 years ago that lysines of histones H3 and H4 can appear in mono-, di- and trimethylated states (hereafter denoted me1, me2 and me3; Paik and Kim, 1971; DeLange *et al*, 1973; Turner, 2005), it has been suggested only recently that these reflect functional differences (Dutnall, 2003). For example, histone H3 can be methylated at different lysine residues, including lysine 4 (K4), lysine (K9) and lysine 27 (K27), and also to different levels at each residue, providing a plethora of combinations. In general, methylation of H3K4 has been associated with transcriptionally active genes (Sims *et al*, 2003). Conversely, methylation of H3K9 has been linked to heterochromatin and gene silencing, typically affecting centromere-associated repeats, arrays of ribosomal RNA genes (rDNA) and transposable elements (Lippman and Martienssen, 2004). In addition to H3K9 methylation, the link between H3K27 methylation and suppressive chromatin has been revealed by enrichment of H3K27me3 at *Hox* genes of *Drosophila* affected by polycomb group protein-mediated silencing (Ringrose and Paro, 2004) and of H3K27me1 at heterochromatic major and minor satellite repeats in mouse (Peters *et al*, 2003). Moreover, the inactive X chromosome in mammals is marked by both H3K9me2 and H3K27me3 (Plath *et al*, 2003; Okamoto *et al*, 2004). Although H3K9me2 was found to be directed to the silent chromosomal regions of plants by hypermethylation of DNA at CpG sites (Soppe *et al*, 2002; Tariq *et al*, 2003), little is known about the role and regulation of H3K27 methylation. Recently, enrichment in H3K9me2 and H3K27me2 has been correlated with inactivation of the *FLC* locus during vernalization (Bastow *et al*, 2004; Sung and Amasino, 2004), but the regulatory relationship between these H3 silencing marks as well as their link to DNA methylation remain unclear.

In plant and mammalian chromosomes, cytosine residues residing in CpG sequence context are modified by the addition of methyl groups and particular patterns of CpG methylation are maintained through DNA replication by the activities of maintenance methyltransferases (Dmmt1 in mammals and MET1 in *Arabidopsis*) (Finnegan and Kovac, 2000; Bird, 2002). Maintenance of CpG methylation is essential for mammalian (Li *et al*, 1992) and plant development (Finnegan *et al*, 1996; Ronemus *et al*, 1996) and important for the perpetuation of chromatin features such as covalent modifications of histones (Johnson *et al*, 2002; Soppe *et al*, 2002; Fuks *et al*, 2003b; Tariq *et al*, 2003; Yan *et al*, 2003). In mammals, H3K9 methylation and CpG methylation show a complex interplay in which each mark can influence the

other (Fuks *et al*, 2003a, b). It has been shown recently that the loss of CpG methylation at pericentromeric repeats results in an increase in H3K4 methylation but has no effect on H3K9 methylation, suggesting independent mechanisms for regulation of K4 and K9 methylation (Yan *et al*, 2003). On the other hand, mouse embryonic stem (ES) cells deficient in *dnmt1* or in the DNA *de novo* methyltransferases *dnmt3a/b* show no alteration in the distribution of H3K9 and H3K27 methylation at tandem or interspersed repeats (Martens *et al*, 2005).

In addition to CpGs, cytosines in CpNpG and CpNpN (N = A, T or C) sequences in plants can also be targeted for methylation by the plant-specific methyltransferase CMT3 (Bartee *et al*, 2001; Lindroth *et al*, 2001). It was shown previously that CpG methylation directs H3K9me2 at pericentromeric repetitive sequences and transposable elements in *Arabidopsis* (Soppe *et al*, 2002; Tariq *et al*, 2003) and that loss of CpG methylation also induces an increase in H3K4me2 at these targets (Tariq *et al*, 2003). The H3K9-specific histone methyltransferase KYP methylates H3K9, which is required for CpNpG methylation via the recruitment of CMT3 (Johnson *et al*, 2002). Recently, it has been suggested that simultaneous methylation of H3 at K9 and K27 is recognized by CMT3, implying that K9 and K27 form a combinatorial histone mark that directs non-CpG methylation and contributes to stabilization of transposable element silencing (Lindroth *et al*, 2004).

Here, we describe the functional relationship of DNA methylation patterns at CpG sites to patterns of H3K27 methylation and compare this to the known relationship between CpG methylation and H3 methylation at K9 and K4. We found unique specificities of the interaction between CpG methylation marks and H3 marked by various K27 methylation levels. These specificities seem to differ between plants and mammals. Most important, our results suggest that changes in CpG methylation influence different histone methylation marks in a non-overlapping and mark-specific manner reflected by the independent redistribution of particular mark(s). This redistribution seems not to be uniform and correlates with transcriptional reactivation of previously silent and CpG hypermethylated targets. Therefore, if epigenetic information encoded by CpG methylation is executed through combinatorial histone code, as proposed by Lindroth *et al* (2004), particular elements of the combinatorial code can be independently regulated, providing an attractive opportunity for the integration of other sources of epigenetic information that may act subsidiary to the CpG methylation blueprint.

Results and discussion

DNA methylation does not determine H3K27me1/me2 patterns

To investigate the functional relationship between CpG methylation and H3K27 methylation patterns, we used a combination of immunostaining and chromatin immunoprecipitation (ChIP) to analyze two *Arabidopsis* mutants (*met1-3* and *ddm1-5*) impaired in the maintenance of CpG methylation patterns (Scheid *et al*, 2002; Saze *et al*, 2003). These are null alleles of either the maintenance methyltransferase 1 (*MET1*) or the DDM1 chromatin-remodeling factor related to *SWI2/SNF2*. Highly specific antibodies able to discriminate methylation levels of histone H3 at lysine 27 were used

(Peters *et al*, 2003; Perez-Burgos *et al*, 2004; Martens *et al*, 2005).

In interphase nuclei of two different *Arabidopsis* ecotypes (*Columbia* and *Zurich*), H3K27me1 and H3K27me2 were both enriched at heterochromatic chromocenters and euchromatin was labeled at a much lower level (Figure 1A and B). Conversely, the antibodies against H3K27me3 specifically labeled euchromatin and were excluded from heterochromatic chromocenters (Figure 1C). Euchromatic H3K27me3 distribution was not homogeneous and speckles with increased signal intensity were visualized. Thus, in our experimental setup, the wild-type distribution of H3K27 methylation marks was identical in the two distinct ecotypes and confirmed the pattern previously observed for the *Columbia* ecotype (Lindroth *et al*, 2004; Naumann *et al*, 2005). Although H3K9me2, H3K27me1 and H3K27me2 were all localized to heterochromatic chromocenters (Figure 1A and B; Probst *et al*, 2003; Tariq *et al*, 2003), H3K9me2

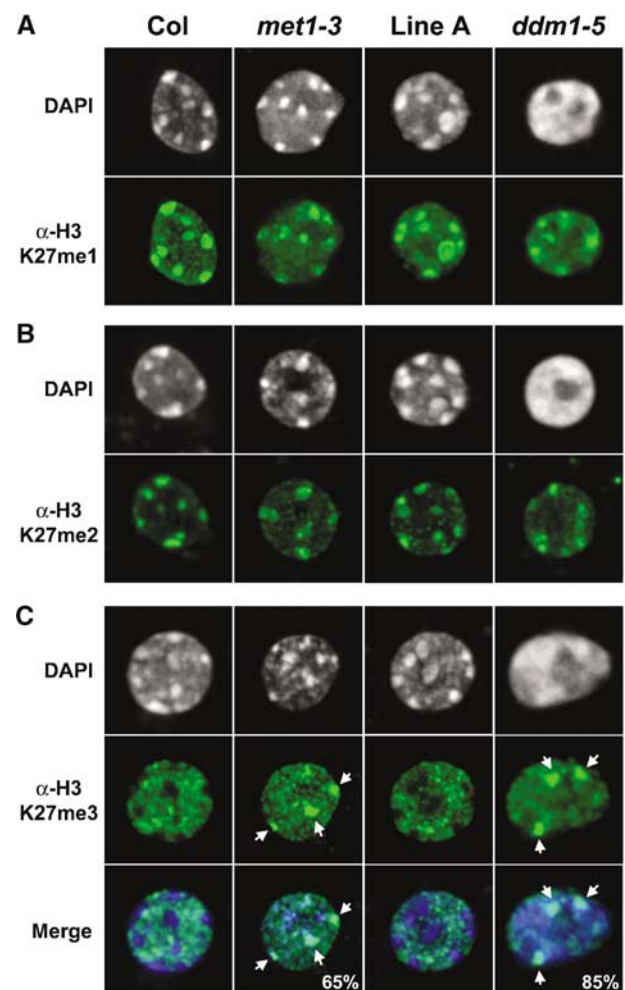


Figure 1 Reduction in DNA methylation affected the distribution of H3K27me3 but not of H3K27me1 and H3K27me2. Immunolocalization experiments (using paraformaldehyde-fixed nuclei) showing the distribution of H3K27me1 (A) H3K27me2 (B) and H3K27me3 (C) in interphase nuclei of wild type (*Columbia* (Col) and *Zurich* (Line A)) and hypomethylated mutants *met1-3* and *ddm1-5*. White arrows in (C) indicate the H3K27me3-enriched foci, and the percent of nuclei showing this staining pattern is indicated. At least 80 nuclei from different preparations were evaluated for each genotype.

was drastically redistributed in *met1-3* (Tariq *et al*, 2003) and *ddm1-5* (Probst *et al*, 2003), but the localization of H3K27me1 and H3K27me2 was not affected by these mutations. Moreover, although the compact structure of centromeric and pericentromeric heterochromatin had largely disintegrated in *ddm1-5* nuclei (Figure 1; Probst *et al*, 2003), H3K27me1 and H3K27me2 staining remained associated with areas similar in distribution and size to those in the wild type (Figure 1A and B). Thus, despite the fact that the heterochromatin structure in *ddm1-5* was disorganized and loosened, the repetitive regions remained enriched in H3K27me1 and me2. Furthermore, although CpG methylation is erased in the *met1-3* strain (Saze *et al*, 2003), there was no change in the association of H3K27me1 and H3K27me2 with heterochromatic chromocenters. These results suggest that CpG methylation states do not significantly influence the distribution of H3K27me1 and H3K27me2, which is in sharp contrast to the prominent impact of CpG methylation on H3K9me2 distribution. CMT3 requires both K9 and K27 methylation marks to be simultaneously present on the same histone H3 N-terminal tail in order to achieve subsequent methylation outside CpGs (Lindroth *et al*, 2004). Because CpG methylation acts upstream of H3K9 methylation in *Arabidopsis* (Soppe *et al*, 2002; Tariq *et al*, 2003), according to the combinatorial histone code hypothesis proposed by Lindroth *et al* (2004), DNA methylation-dependent changes in the distribution of the heterochromatin-specific H3 marks (K9me2 and K27me1 or K27me2) would be expected to be more synchronous. In contrast, our results clearly favor the autonomy of H3K27me1/me2 patterns in relation to DNA methylation and H3K9me2 (see below). Such autonomy of K9 and K27 regulation provides an opportunity for the combinatorial histone code to integrate still unknown signals in addition to CpG methylation that would act upon upstream CMT3-mediated CpNpG methylation, through changes in H3K27me1/me2. At present, however, the combinatorial histone code proposition involving simultaneous H3 methylation in the K9 and K27 positions is somewhat uncertain due to the use in the *in vitro* binding assays of synthetic H3 peptides doubly trimethylated at K9 and K27, which both represent euchromatic marks (Lindroth *et al*, 2004; Naumann *et al*, 2005; see below). As a consequence, the functional cooperation between K9 and K27 methylation marks in *Arabidopsis* remains unclear.

Target-specific enrichment of H3K27me3 upon loss of CpG methylation

In contrast to the remarkable stability of H3K27me1 and H3K27me2 marks in *met1-3* and *ddm1-5*, we observed very specific alterations in H3K27me3 distribution in both mutants. In the corresponding wild types, H3K27me3 was localized to euchromatin and in both mutants H3K27me3 immunostaining was largely relocated into selected heterochromatic regions, revealing two to four foci with prominent signals that colocalized with a subset of chromocenters (Figure 1C). Since 8–10 chromocenters on average are visualized in DAPI-stained *Arabidopsis* interphase nuclei, which are all hypomethylated in DNA methylation-deficient mutants (Probst *et al*, 2003; Saze *et al*, 2003; Tariq *et al*, 2003), it became obvious that the redistribution of H3K27me3 does not simply follow DNA methylation changes but is reinforced by a more complex mechanism.

To investigate this, we compared H3K27me1, H3K27me2 and H3K27me3 distribution at specific targets in wild-type and *met1-3* or *ddm1-5* plants by ChIP (Figure 2A; the data for *ddm1-5* are not shown, since both DNA hypomethylation mutants yielded similar results). The immunocytology data showed enhanced accumulation of H3K27me3 at two to four foci colocalizing with heterochromatin and initially indicated that the 45S rDNA repeats are possible targets, since 45S rDNA repeats are located at heterochromatic domains of only chromosomes 2 and 4 (Maluszynska and Heslop-Harrison, 1991). However, the levels of H3K27 methylation at 45S rDNA, also including trimethylation, were not affected in *met1-3* (Figure 2A and B) or in *ddm1-5* plants (data not shown). Therefore, the elevated H3K27me3 signals observed in both mutants do not correspond to the 45S rDNA repeats. Next, we examined H3K27 methylation distribution at the 180 bp centromeric repeats present on all chromosomes. Again, the wild-type H3K27 methylation patterns were not altered in *met1-3* or *ddm1-5* (Figure 2 and data not shown).

Since not all chromocenters of the mutants were equally enriched in H3K27me3, we determined whether a particular subset of centromeric repeats could be selectively affected. Primers that specifically amplify a particular 180 bp repeat (GenBank accession no. AB062092, nucleotides 88433–88939) residing within the heterochromatin block of chromosome 1 were used. This repeat was previously shown to be completely depleted of CpG methylation in the *met1-3* mutant (Saze *et al*, 2003). In wild-type plants, H3K27 methylation patterns of this sequence were equivalent to those observed for other centromeric 180 bp repeats. However, the association of this sequence with H3K27me3 was increased more than four-fold in *met1-3* and *ddm1-5* (Figure 2A and B and data not shown), suggesting that only specific 180 bp repeats gain H3K27me3 upon demethylation of DNA. Cytosine methylation assay using CpG methylation-sensitive restriction endonuclease digestion followed by PCR confirmed that CpG methylation is erased at this locus in *met1-3* (Figure 3; Saze *et al*, 2003).

Chromocenters are enriched in various types of transposable elements (The Arabidopsis Genome Initiative, 2000) and the 180 bp repeat that gained H3K27me3 is flanked by sequences related to transposable elements. Therefore, we extended our analysis to a selection of pericentromeric sequences annotated as putative transposable elements (*CACTA-like* At4g03745, *Ta2* At4g06488, *Ta3* At1g37110, *TSI* and *MULE* At4g03870) or putative transposable elements residing outside of chromocenters within a euchromatin environment (*AtSN1* located between At3g44000 and At3g44005, and *MULE* At2g15810). Interestingly, all but *MULE* At4g03870 showed a significant enrichment in H3K27me3 in *met1-3* and *ddm1-5* (2- to 25-fold; Figure 2A and B and data not shown) although CpG methylation was strongly reduced at all these targets (Figure 3). Notably, the levels and patterns of H3K27me1 and me2 remained unchanged at both euchromatic and heterochromatic targets in agreement with the cytological data. Moreover, it has been shown that upon vernalization, the transcriptional down-regulation of the *FLC* locus is correlated with an enrichment in H3K27me2, but no change in DNA methylation was observed (Bastow *et al*, 2004; Sung and Amasino, 2004). This supports the autonomy of H3K27me1/me2 in relation to DNA methylation.

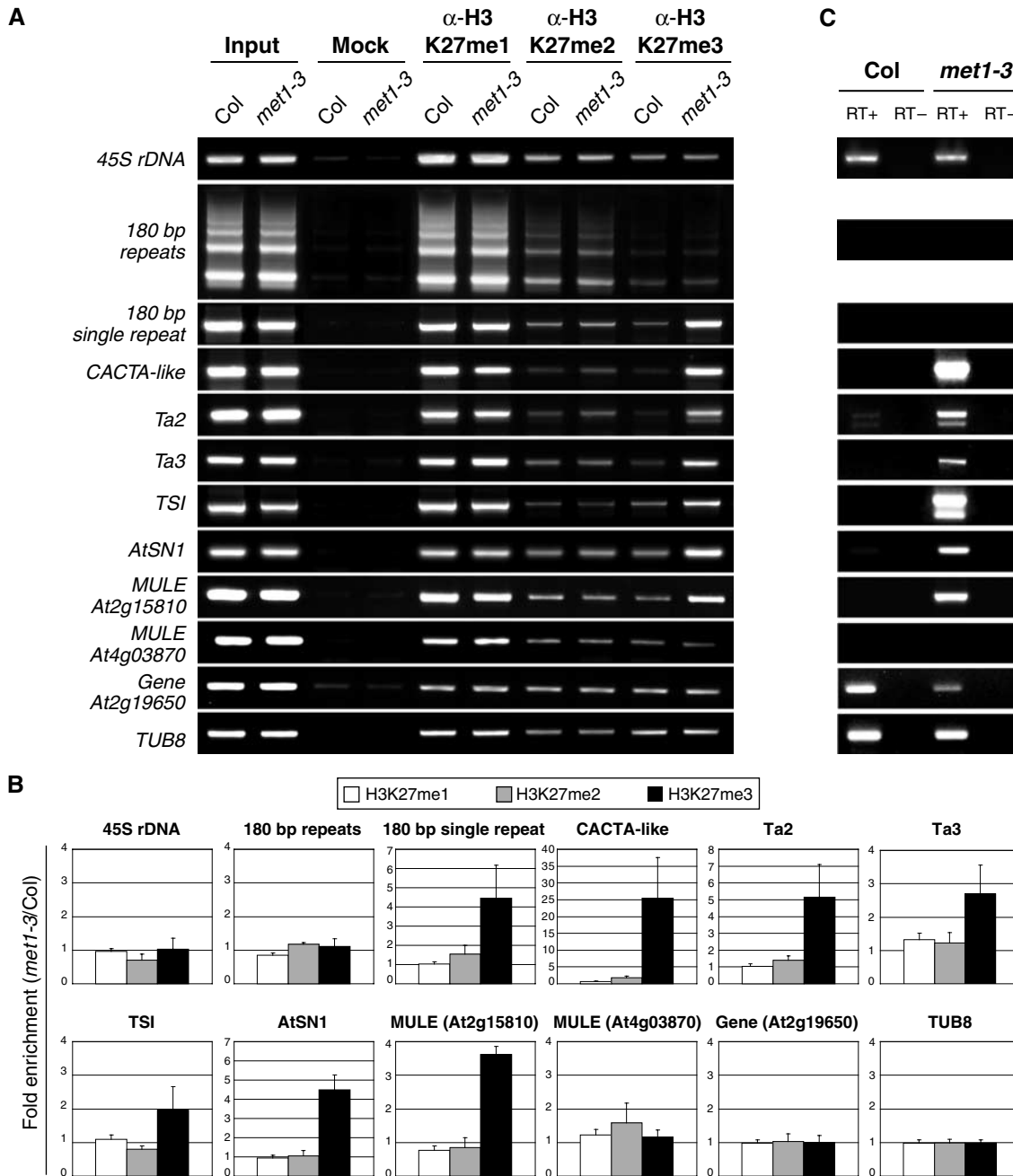


Figure 2 Depletion of DNA methylation induced enrichment in H3K27me3 correlating with transcriptional reactivation. (A) ChIP analysis using antibodies specific for the three H3K27 methylation states (me1, me2 and me3). Representative gel pictures of three independent replicates are shown. (B) Fold enrichment of a particular sequence in the pull-down of *met1-3* versus wild type, normalized by the amplification of *Tubulin8* (*TUB8*) and *Actin2/7* genes. No changes in the H3K27 methylation patterns for the euchromatic genes *TUB8* and *ACTIN2/7* were observed when comparing equal amounts of tissues. The results of three independent ChIP experiments are shown and the standard error of the mean is indicated on each bar. (C) RT-PCR analysis of transcripts with (+) and without (-) reverse transcriptase (RT).

Enrichment of H3K27me3 correlates with transcriptional reactivation

To determine why the transposable elements were not all enriched in H3K27me3 in the mutants, we examined their transcriptional activity using total cellular and polyadenylated RNA. In general, genes already active in the wild type retained association with H3K27me3 in the mutants and did not become further enriched in this histone mark upon genome-wide DNA demethylation (Figure 2). On the other hand, transcriptional reactivation of previously silent targets

in *met1-3* and *ddm1-5* correlated well with enrichment in H3K27me3 (Figure 2C and data not shown). However, we were not able to detect transcripts originating from the 180 bp single repeat using RT-PCR from total RNA preparations. Interestingly, this repeat is directly flanked 5' by an LTR of a putative transposon (GenBank accession no. AB062092, nucleotides 87 599–88 432). RT-PCR assays using primers specific to this LTR revealed transcriptional reactivation of the LTR in both mutants (data not shown). Thus, enrichment of H3K27me3 may have been linked to transcriptional

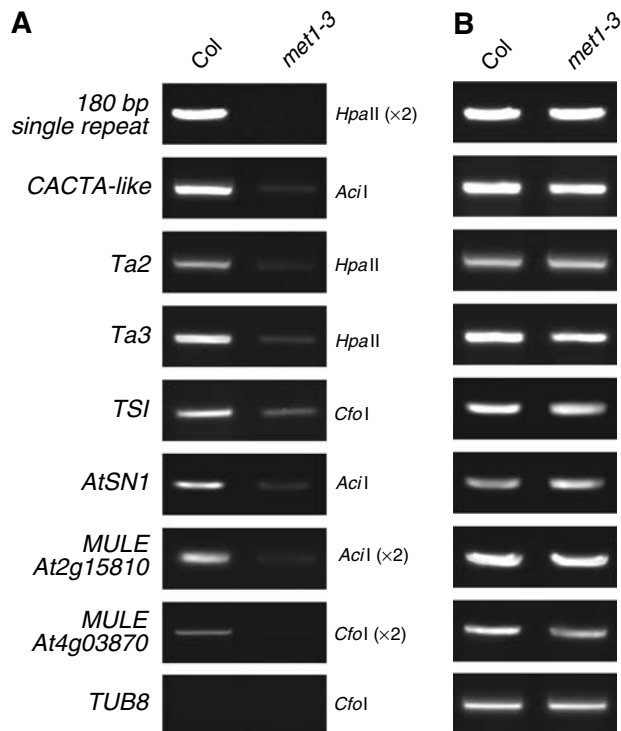


Figure 3 *met1-3* mutation caused drastic reduction in CpG methylation. (A) Targets were PCR amplified using primer pairs used in Figure 2, after digestion of the DNA with the restriction enzymes indicated ($\times 2$ indicates that two restriction sites are present). (B) Undigested DNA served as PCR control.

reactivation also in this case and the H3K27me3 mark may have spread into adjacent, silent DNA of the 180 bp repeat.

Specific 5S rDNA pericentromeric repeats gain H3K27me3 upon DNA demethylation

Since homologs of the analyzed transposable element targets are found in the pericentromeric regions of all chromosomes, their enrichment in H3K27me3 does not explain the formation of two to four strong signals in the mutant nuclei. To search for an explanation, we focused our attention on heavily methylated 5S rDNA genes, which reside at the pericentromeric regions of chromosomes 3, 4 and 5 in *Arabidopsis*, amounting to over one thousand copies (the 5S rDNA locus on chromosome 3 is absent in the *Zurich* ecotype). Fluorescent *in situ* hybridization (FISH) with a 5S probe produced signals that colocalized with a subset of chromocenters (Fransz *et al*, 2002; Mathieu *et al*, 2003; Figure 4B). Furthermore, only 5S gene arrays on chromosome 4 and/or 5 are transcriptionally active (Cloix *et al*, 2002). It therefore was plausible that changes in histone methylation status at 5S rDNA in *met1-3* and *ddm1-5* caused the intensely labeled H3K27me3-specific foci. Indeed, ChIP analysis showed that these repeats become enriched in H3K27me3 up to five-fold in both *ddm1-5* and *met1-3* (Figure 4A), while H3K27me1 and H3K27me2 methylation patterns again were unaffected. A combination of H3K27me3 immunostaining and DNA FISH for 5S rDNA repeats revealed that one ($\sim 98\%$ of nuclei) and rarely two ($\sim 2\%$ of nuclei) 5S gene arrays colocalized with the H3K27me3-specific foci (Figure 4B). Therefore, the enrichment of H3K27me3 at 5S rDNA repeats, although remarkably specific, did not provide

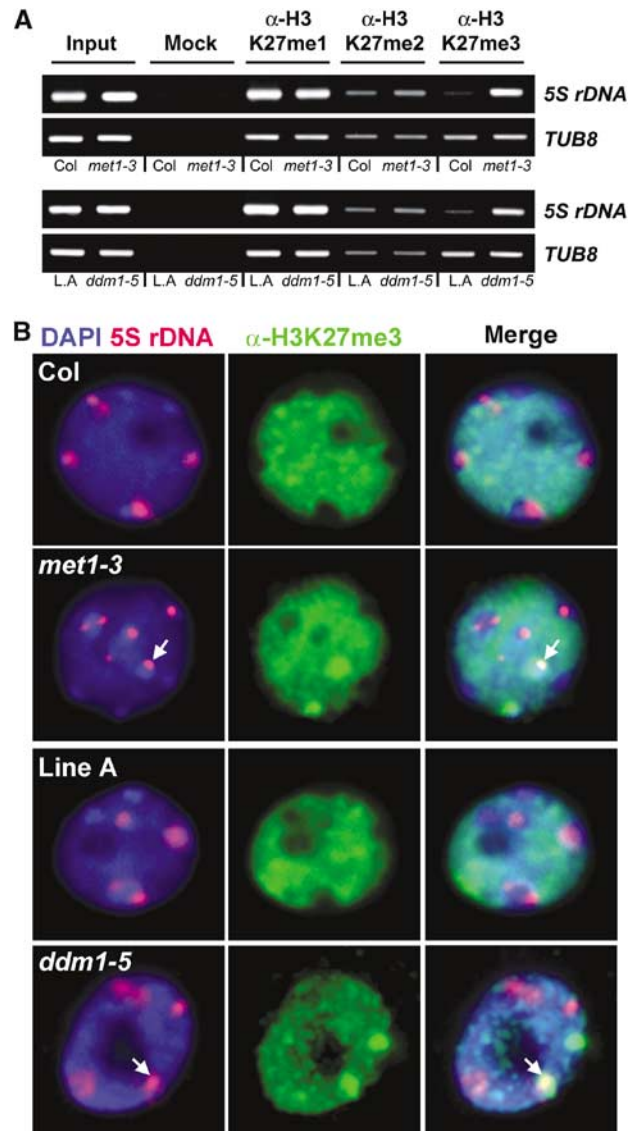


Figure 4 5S rDNA repeats became specifically enriched in H3K27me3 and contributed partly to the appearance of H3K27me3-enriched spots in DNA hypomethylation mutants. (A) ChIP analysis using antibodies specific for the three H3K27 methylation states (me1, me2 and me3). Representative gel pictures of three independent replicates are shown. (B) Immuno-DNA FISH results revealing the colocalization (white arrows) of a selection of 5S rDNA loci with chromatin foci enriched in H3K27me3 in *met1-3* and *ddm1-5* interphase nuclei.

a full explanation for the observed H3K27me3 labeling pattern in the mutant nuclei. 5S rDNA blocks free of H3K27me3-specific foci and also H3K27me3 enrichment foci outside the 5S rDNA arrays were also observed. Both mutants were shown to reactivate the transcription of silent minor 5S rDNA genes (Mathieu *et al*, 2003; O Mathieu, unpublished results), reinforcing the conclusion that the enrichment of H3K27me3 is correlated with transcriptional reactivation of previously silenced repeats. In fact, it is possible that only 5S genes gaining transcriptional activity acquire H3K27me3, and that this involves only one 5S rDNA array (e.g. only one of the two chromosomes 5). Thus, 5S rDNA loci might be the subject of parent of origin epigenetic regulation, which is revealed in *met1-3* and *ddm1-5* backgrounds through the locus-specific enrichment of the

H3K27me3. More detailed studies are needed to resolve this issue. Nevertheless, we have demonstrated a clear link between a reduction in DNA methylation at various pericentromeric repeats, including 5S rDNA, and a gain in H3K27me3.

H3K9me2 and H3K27 methylation are independent epigenetic marks

Previously, we reported pericentromeric depletion of the heterochromatic H3 mark K9me2 in the *met1-3* mutant (Tariq *et al*, 2003). Since this was observed at several of the heterochromatic targets analyzed in the present study, we investigated whether enrichment of H3K27me3 was a direct consequence of CpG methylation depletion or was a secondary effect of the decrease in H3K9me2 at these target sequences. To address this issue, we analyzed the distribution of H3K27 mono-, di- and trimethylation in the *kyp* mutant. The *KYP* gene encodes an H3K9-specific histone methyltransferase and its mutation has been shown to reduce H3K9me2 levels at various target sequences, including the centromeric 180 bp repeats and the *Ta2* and *Ta3* retrotransposons analyzed here (Johnson *et al*, 2002, 2004). Notably, the *kyp* mutation had no influence on H3K27 methylation patterns at any of the 13 targets assayed, located either in euchromatin or in heterochromatin, providing evidence that *KYP*-mediated H3K9me2 does not influence H3K27 methylation (Figure 5A). This is in agreement with the previous observation of H3K27 methylation pattern (me1, me2 and me3) stability at the 180 bp *CEN* repeats and the *Ta3* retrotransposon in *kyp* (Lindroth *et al*, 2004) as well as *met1-3* and *ddm1-5* (Figure

2A and B and data not shown). However, our results also suggest that changes in H3K27me3 induced by DNA hypomethylation are not a consequence of the reduction of H3K9me2 at the affected targets. In addition, Naumann *et al* (2005) reported that H3K27 methylation patterns were not affected in two mutant alleles of *KYP*. The interpretation of this observation is unclear, however, given that no H3K9me2 reduction was observed at chromocenters of these two *kyp* alleles, oppositely to previous reports (Jasencakova *et al*, 2003; Jackson *et al*, 2004) and to our data (Figure 5B). Interestingly, in contrast to our observations in *Arabidopsis*, ES cells deficient in *dnmt1* or the *de novo* DNA methyltransferases *dnmt3a/b* showed no alteration in the distribution of either histone H3K9 or H3K27 methylation at mouse tandem or interspersed repeats, while major satellites showed a loss of H3K27me1 and an increase in H3K27me3 in ES cells deficient for histone H3K9 methyltransferase *suv39h* (Martens *et al*, 2005). Our data suggest that as in *Drosophila* (Ebert *et al*, 2004), in *Arabidopsis* also H3K9 and H3K27 methylation do not represent interdependent repressive marks, although they appear to be functionally interconnected in the establishment of repressive heterochromatic structures and gene silencing in both organisms.

CpG methylation directly restrains H3K4me2 independently of H3K9me2

H3K27me3 and H3K4me2 are both euchromatic marks in plants. We have shown that the heterochromatic mark

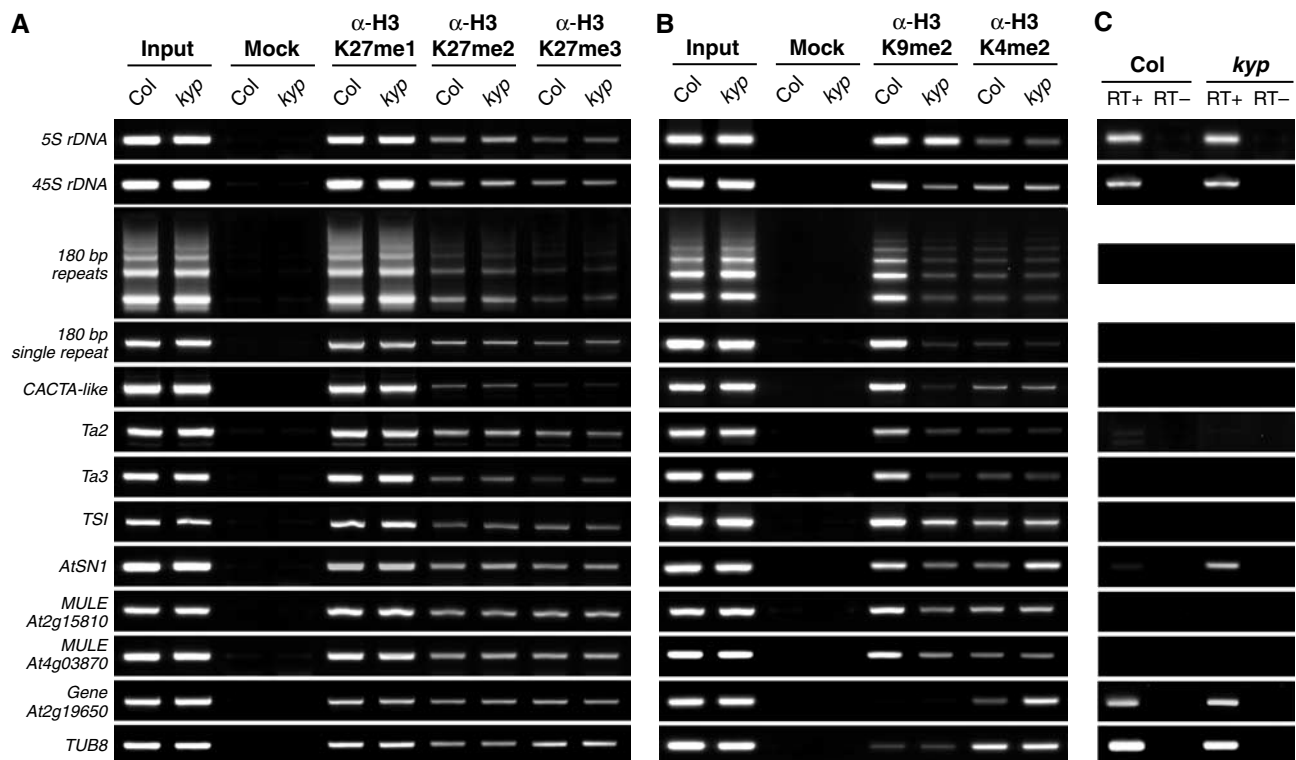


Figure 5 Reduction of H3K9me2 methylation in the *kyp* mutant did not affect the distribution of H3K27 methylation states and induced an increase in H3K4me2 only in a transcription-dependent manner. (A) ChIP analysis using antibodies specific for the three H3K27 methylation states (me1, me2 and me3) in Columbia (Col) wild-type and *kyp* plants. Representative gel pictures of three independent replicates are shown. (B) ChIP analysis using antibodies against H3K9me2 and H3K4me2 in Col and *kyp* plants. (C) RT-PCR analysis of transcripts with (+) and without (-) reverse transcriptase (RT).

H3K9me2 does not determine H3K27 methylation patterns. However, the decrease in H3K9me2 observed in *ddm1* and *met1* also correlates with a gain in H3K4me2 at pericentromeric repeats and transposable elements (Gendrel *et al*, 2002; Tariq *et al*, 2003). This enrichment in H3K4me2 could be due to loss of CpG methylation, or it could be an indirect consequence of the decrease in H3K9me2. To assess whether H3K9me2 competes with H3K4me2, we compared H3K4me2 patterns in wild-type and *kyp* plants. Despite the major reduction in H3K9me2 at the analyzed targets, H3K4me2 increased only at *AtSN1* and the gene *At2g19650* (Figure 5B). Our ChIP data confirm and extend a previous report showing, by immunostaining, that H3K4me2 pattern was similar in *kyp* and wild-type plant nuclei (Jasencakova *et al*, 2003). Together, this indicates that H3K9me2 in general does not restrain H3K4me2. However, since *AtSN1* and *At2g19650* were both found to be transcriptionally active in *kyp* (Figure 5C), we formulate the hypothesis that H3K9me2 may influence H3K4me2 in a transcription-dependent manner at specific euchromatin target sequences, which is best illustrated here by H3 methylation changes at *AtSN1*. Notably, H3K9me2 levels were not affected at 5S rDNA in *kyp*, indicating that H3K9me2 at these repeats is maintained by another histone methyltransferase (Figure 5B). However, this putative 5S rDNA-specific histone methyltransferase, like KYP, requires a CpG methylation signal, since in the *met1-3* mutant we observed depletion of H3K9me2 at 5S rDNA (data not shown). Therefore, together with the observed increase in H3K27me3 at 5S rDNA in the *met1-3* mutant, this finding reinforces our previous conclusion that CpG methylation directly restrains H3K27me3 and is required in parallel for the establishment of H3K9me2.

Conclusion

Our data highlight the importance of CpG methylation in providing a scaffold for a subset of modifications of H3 (K4me2, K9me2 and K27me3); however, H3K27me1 and H3K27me2 are not affected by changes in CpG methylation (Figure 6). It is possible that other factors regulate the distribution of H3K27me1 and H3K27me2 in *Arabidopsis* and the combination of H3 methylation marks may indeed contribute to the higher order of epigenetic information necessary for the recognition of additional epigenetic regulators, as proposed for CMT3 (Lindroth *et al*, 2004). In this case, the proper recruitment of such factors may be regulated by CpG methylation patterns in conjunction with other cues influencing corresponding additional histone modification.

Moreover, although CpG methylation is an important player in the self-reinforcing loop of chromatin-mediated epigenetic regulation in plants and mammals, it is apparent that the use and the meaning of particular epigenetic marks within this loop differ significantly between these organisms. For example, H3K9me1 and me2 are two marks of euchromatin in mammals, but are associated with heterochromatin in *Arabidopsis*. Also, H3K27me2 and me3 are enriched at euchromatin and heterochromatin, respectively, in mammals, but the converse is true for *Arabidopsis*. This indicates that the epigenetic code itself may be evolutionarily conserved, but that the functional meaning of its elements has probably evolved separately in different organisms.

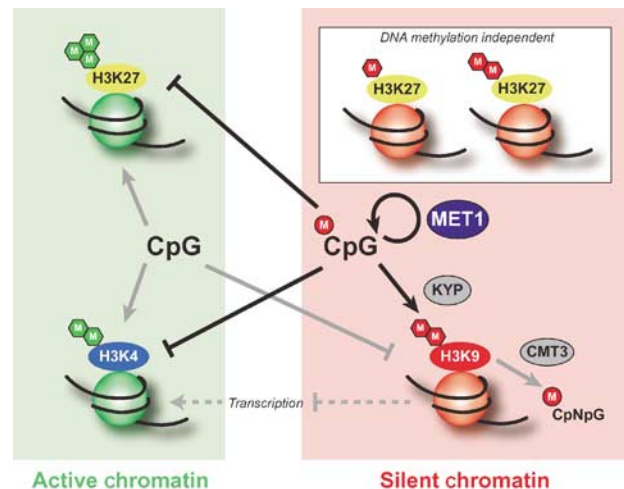


Figure 6 Summary of the influence of CpG methylation on distinct histone H3 modifications in *Arabidopsis*. CpG methylation maintained by MET1 represses H3K27me3 and H3K4me2, which mark active chromatin. Conversely, methylated CpGs stimulate H3K9me2, a hallmark of silent chromatin, which in turn can induce CpNpG methylation via the chromomethylase CMT3. At some specific target sequences, H3K9me2 may also restrain H3K4me2 in a transcription-dependent manner (dotted lines). The heterochromatin marks H3K27me1 and H3K27me2 are not influenced by DNA methylation and are modulated by as yet unknown factors.

Materials and methods

Plant material

Plants were grown in soil in a growth chamber under short-day conditions (12 h light/12 h dark at 22°C). The *met1-3* strain contained a T-DNA insertion disrupting the conserved DNA methyltransferase motif region of MET1 (Saze *et al*, 2003). The *ddm1-5* (*som8*) mutant has been described previously (Mittelsten Scheid *et al*, 1998; Jeddloh *et al*, 1999) and the *kyp* T-DNA insertion line (SALK_069326) was obtained from the SALK Institute Genomic Analysis Laboratory.

Immunostaining

Immunostaining experiments were performed with young rosette leaves as described (Probst *et al*, 2004). Slides were incubated overnight at 4°C with antibodies against mono-, di- and trimethyl H3K27 (Perez-Burgos *et al*, 2004; dilution 1:100) in 1% BSA in PBS. Detection was performed with an anti-rabbit Alexa 488-coupled antibody (1:100, 37°C, 1 h; Molecular Probes) in 0.5% BSA in PBS. DNA was counterstained with DAPI in Vectashield mounting medium (Vector Laboratories).

For the combined detection of histone H3 modifications and 5S rDNA, immunodetection was performed, and the slides were further processed for subsequent FISH as described (Probst *et al*, 2004). A biotin-16-dUTP-labeled 5S rDNA probe was generated by PCR using the 5S rRNA gene-specific primers 5S1 and 5S2 (see Supplementary Table 1). Images were analyzed with a Zeiss Axioplan 2 microscope equipped with a cooled charge-coupled device camera. Image stacks were deconvoluted with AutoDeblur-software (AutoQuant) and single layers were chosen for illustration. Images were merged and processed using Adobe Photoshop (Adobe Systems).

Chromatin immunoprecipitation

ChIP was performed as described previously (Gendrel *et al*, 2002; Johnson *et al*, 2002; Probst *et al*, 2004) with minor modifications. The histone-DNA complexes were immunoprecipitated with α -mono-, α -di-, α -trimethyl H3K27, α -dimethyl H3K9 (Perez-Burgos *et al*, 2004) and α -dimethyl H3K4 antibodies (Upstate Biotechnology). After reverse crosslinking and proteinase K treatment, the immunoprecipitated DNA was purified using a silica-gel membrane (Qiagen) and analyzed by PCR. All PCR reactions were performed in 20 μ l, starting with 5 min at 95°C and followed by 21–40 cycles

(depending on the region being amplified) of 95°C, 60°C (50°C for 45S rDNA and 54°C for 5S rDNA) and 72°C (30 s each) with a final elongation of 5 min at 72°C. PCR products were scanned with a Molecular Imager FX (Bio-Rad) after electrophoretic separation and quantified using the Quantity One software (Bio-Rad). Target amplifications were normalized for amplification of the *Tubulin8* gene. Identical results were obtained using amplification of the *Actin2/7* gene as a reference. Primer sequences are listed in Supplementary Table 1.

Cytosine methylation assay

Genomic DNA (1 µg) was digested with the CpG methylation-sensitive restriction endonucleases *AclI*, *CfoI* or *HpaII*. Undigested DNA was used as a control. Approximately 20 ng of DNA was then used for each PCR reaction. All PCR reactions were performed in 20 µl, starting with 5 min at 95°C and followed by 30 cycles of 95, 60 and 72°C (45 s each) with a final elongation of 5 min at 72°C. PCR products were subjected to agarose gel electrophoresis. Primer sequences are listed in Supplementary Table 1.

RT-PCR

RNA was isolated from leaf tissues (as for ChIP) using the TRI-reagent (Sigma) according to the manufacturer's instructions. Aliquots of 1 µg of total RNA treated with DNase (Invitrogen) were

reverse transcribed using an oligo(dT)-anchored primer (Invitrogen) and cDNA was PCR amplified for 30 cycles (94°C for 30 s, 60°C for 30 s and 72°C for 30 s) with gene-specific primers. For *AtSN1* expression analysis, 100 ng DNase-treated total RNA was used as input in RT-PCR reactions using the OneStep RT-PCR kit (Qiagen); RT-PCR conditions were as described (Herr *et al*, 2005). 5S rRNA, 45S rRNA and LTR (GenBank accession no. AB062092, nucleotides 87 599–88 432) cDNAs were synthesized and amplified for 20 (5S and 45S repeats) or 40 (LTR) cycles using the procedure described for *AtSN1*. Amplification of *Tub8* RNA was used as an internal control in each case. Primer sequences are listed in Supplementary Table 1.

Supplementary data

Supplementary data are available at *The EMBO Journal* Online.

Acknowledgements

We thank T Jenuwein for providing antibodies as part of The Epigenome—Network of Excellence (NoE), and S Takeda, P King and S Guimil for helpful comments on the manuscript. This work was supported by the European Commission through The Epigenome—Network of Excellence (LSHG-CT-2004-503433).

References

- Bartee L, Malagnac F, Bender J (2001) *Arabidopsis* cmt3 chromomethylase mutations block non-CG methylation and silencing of an endogenous gene. *Genes Dev* **15**: 1753–1758
- Bastow R, Mylne JS, Lister C, Lippman Z, Martienssen RA, Dean C (2004) Vernalization requires epigenetic silencing of FLC by histone methylation. *Nature* **427**: 164–167
- Berger SL (2002) Histone modifications in transcriptional regulation. *Curr Opin Genet Dev* **12**: 142–148
- Bird A (2002) DNA methylation patterns and epigenetic memory. *Genes Dev* **16**: 6–21
- Cloix C, Tutois S, Yukawa Y, Mathieu O, Cuveillier C, Espagnol MC, Picard G, Tourmente S (2002) Analysis of the 5S RNA pool in *Arabidopsis thaliana*: RNAs are heterogeneous and only two of the genomic 5S loci produce mature 5S RNA. *Genome Res* **12**: 132–144
- DeLange RJ, Hooper JA, Smith EL (1973) Histone 3. 3. Sequence studies on the cyanogen bromide peptides; complete amino acid sequence of calf thymus histone 3. *J Biol Chem* **248**: 3261–3274
- Dutnall RN (2003) Cracking the histone code: one, two, three methyls, you're out!. *Mol Cell* **12**: 3–4
- Ebert A, Schotta G, Lein S, Kubicek S, Krauss V, Jenuwein T, Reuter G (2004) Su(var) genes regulate the balance between euchromatin and heterochromatin in *Drosophila*. *Genes Dev* **18**: 2973–2983
- Finnegan EJ, Kovac KA (2000) Plant DNA methyltransferases. *Plant Mol Biol* **43**: 189–201
- Finnegan EJ, Peacock WJ, Dennis ES (1996) Reduced DNA methylation in *Arabidopsis thaliana* results in abnormal plant development. *Proc Natl Acad Sci USA* **93**: 8449–8454
- Fransz P, De Jong JH, Lysak M, Castiglione MR, Schubert I (2002) Interphase chromosomes in *Arabidopsis* are organized as well defined chromocenters from which euchromatin loops emanate. *Proc Natl Acad Sci USA* **99**: 14584–14589
- Fuks F, Hurd PJ, Deplus R, Kouzarides T (2003a) The DNA methyltransferases associate with HP1 and the SUV39H1 histone methyltransferase. *Nucleic Acids Res* **31**: 2305–2312
- Fuks F, Hurd PJ, Wolf D, Nan X, Bird AP, Kouzarides T (2003b) The methyl-CpG-binding protein MeCP2 links DNA methylation to histone methylation. *J Biol Chem* **278**: 4035–4040
- Gendrel AV, Lippman Z, Yordan C, Colot V, Martienssen RA (2002) Dependence of heterochromatic histone H3 methylation patterns on the *Arabidopsis* gene DDM1. *Science* **297**: 1871–1873
- Herr AJ, Jensen MB, Dalmay T, Baulcombe DC (2005) RNA polymerase IV directs silencing of endogenous DNA. *Science* **308**: 118–120
- Jackson JP, Johnson L, Jasencakova Z, Zhang X, PerezBurgos L, Singh PB, Cheng X, Schubert I, Jenuwein T, Jacobsen SE (2004) Dimethylation of histone H3 lysine 9 is a critical mark for DNA methylation and gene silencing in *Arabidopsis thaliana*. *Chromosoma* **112**: 308–315
- Jasencakova Z, Soppe WJ, Meister A, Gernand D, Turner BM, Schubert I (2003) Histone modifications in *Arabidopsis*—high methylation of H3 lysine 9 is dispensable for constitutive heterochromatin. *Plant J* **33**: 471–480
- Jeddeloh JA, Stokes TL, Richards EJ (1999) Maintenance of genomic methylation requires a SWI2/SNF2-like protein. *Nat Genet* **22**: 94–97
- Jenuwein T, Allis CD (2001) Translating the histone code. *Science* **293**: 1074–1080
- Johnson L, Cao X, Jacobsen S (2002) Interplay between two epigenetic marks. DNA methylation and histone H3 lysine 9 methylation. *Curr Biol* **12**: 1360–1367
- Li E, Bestor TH, Jaenisch R (1992) Targeted mutation of the DNA methyltransferase gene results in embryonic lethality. *Cell* **69**: 915–926
- Lindroth AM, Cao X, Jackson JP, Zilberman D, McCallum CM, Henikoff S, Jacobsen SE (2001) Requirement of CHROMOMETHYLASE3 for maintenance of CpXpG methylation. *Science* **292**: 2077–2080
- Lindroth AM, Shultis D, Jasencakova Z, Fuchs J, Johnson L, Schubert D, Patnaik D, Pradhan S, Goodrich J, Schubert I, Jenuwein T, Khorasanizadeh S, Jacobsen SE (2004) Dual histone H3 methylation marks at lysines 9 and 27 required for interaction with CHROMOMETHYLASE3. *EMBO J* **23**: 4286–4296
- Lippman Z, Martienssen R (2004) The role of RNA interference in heterochromatic silencing. *Nature* **431**: 364–370
- Maluszynska J, Heslop-Harrison JS (1991) Localization of tandemly repeated DMA sequences in *Arabidopsis thaliana*. *Plant J* **1**: 159–166
- Martens JH, O'Sullivan RJ, Braunschweig U, Opravil S, Radolf M, Steinlein P, Jenuwein T (2005) The profile of repeat-associated histone lysine methylation states in the mouse epigenome. *EMBO J* **24**: 800–812
- Mathieu O, Jasencakova Z, Vaillant I, Gendrel AV, Colot V, Schubert I, Tourmente S (2003) Changes in 5S rDNA chromatin organization and transcription during heterochromatin establishment in *Arabidopsis*. *Plant Cell* **15**: 2929–2939
- Mittelsten Scheid O, Afsar K, Paszkowski J (1998) Release of epigenetic gene silencing by *trans*-acting mutations in *Arabidopsis*. *Proc Natl Acad Sci USA* **95**: 632–637
- Naumann K, Fischer A, Hofmann I, Krauss V, Phalke S, Irmeler K, Hause G, Aurich AC, Dorn R, Jenuwein T, Reuter G (2005) Pivotal role of AtSUVH2 in heterochromatic histone methylation and gene silencing in *Arabidopsis*. *EMBO J* **24**: 1418–1429
- Okamoto I, Otte AP, Allis CD, Reinberg D, Heard E (2004) Epigenetic dynamics of imprinted X inactivation during early mouse development. *Science* **303**: 644–649
- Paik WK, Kim S (1971) Protein methylation. *Science* **174**: 114–119

- Perez-Burgos L, Peters AH, Opravil S, Kauer M, Mechtler K, Jenuwein T (2004) Generation and characterization of methyl-lysine histone antibodies. *Methods Enzymol* **376**: 234–254
- Peters AH, Kubicek S, Mechtler K, O'Sullivan RJ, Derijck AA, Perez-Burgos L, Kohlmaier A, Opravil S, Tachibana M, Shinkai Y, Martens JH, Jenuwein T (2003) Partitioning and plasticity of repressive histone methylation states in mammalian chromatin. *Mol Cell* **12**: 1577–1589
- Plath K, Fang J, Mlynarczyk-Evans SK, Cao R, Worringer KA, Wang H, de la Cruz CC, Otte AP, Panning B, Zhang Y (2003) Role of histone H3 lysine 27 methylation in X inactivation. *Science* **300**: 131–135
- Probst AV, Fagard M, Proux F, Mourrain P, Boutet S, Earley K, Lawrence RJ, Pikaard CS, Murfett J, Furner I, Vaucheret H, Scheid OM (2004) *Arabidopsis* histone deacetylase HDA6 is required for maintenance of transcriptional gene silencing and determines nuclear organization of rDNA repeats. *Plant Cell* **16**: 1021–1034
- Probst AV, Fransz PF, Paszkowski J, Scheid OM (2003) Two means of transcriptional reactivation within heterochromatin. *Plant J* **33**: 743–749
- Ringrose L, Paro R (2004) Epigenetic regulation of cellular memory by the Polycomb and Trithorax group proteins. *Annu Rev Genet* **38**: 413–443
- Ronemus MJ, Galbiati M, Ticknor C, Chen J, Dellaporta SL (1996) Demethylation-induced developmental pleiotropy in *Arabidopsis*. *Science* **273**: 654–657
- Saze H, Scheid OM, Paszkowski J (2003) Maintenance of CpG methylation is essential for epigenetic inheritance during plant gametogenesis. *Nat Genet* **34**: 65–69
- Scheid OM, Probst AV, Afsar K, Paszkowski J (2002) Two regulatory levels of transcriptional gene silencing in *Arabidopsis*. *Proc Natl Acad Sci USA* **99**: 13659–13662
- Sims III RJ, Nishioka K, Reinberg D (2003) Histone lysine methylation: a signature for chromatin function. *Trends Genet* **19**: 629–639
- Soppe WJ, Jasencakova Z, Houben A, Kakutani T, Meister A, Huang MS, Jacobsen SE, Schubert I, Fransz PF (2002) DNA methylation controls histone H3 lysine 9 methylation and heterochromatin assembly in *Arabidopsis*. *EMBO J* **21**: 6549–6559
- Sung S, Amasino RM (2004) Vernalization in *Arabidopsis thaliana* is mediated by the PHD finger protein VIN3. *Nature* **427**: 159–164
- Tariq M, Saze H, Probst AV, Lichota J, Habu Y, Paszkowski J (2003) Erasure of CpG methylation in *Arabidopsis* alters patterns of histone H3 methylation in heterochromatin. *Proc Natl Acad Sci USA* **100**: 8823–8827
- The Arabidopsis Genome Initiative (2000) Analysis of the genome sequence of the flowering plant *Arabidopsis thaliana*. *Nature* **408**: 796–815
- Turner BM (2005) Reading signals on the nucleosome with a new nomenclature for modified histones. *Nat Struct Mol Biol* **12**: 110–112
- Yan Q, Huang J, Fan T, Zhu H, Muegge K (2003) Lsh, a modulator of CpG methylation, is crucial for normal histone methylation. *EMBO J* **22**: 5154–5162